

Early anthropogenic impact on Western Central African rainforests 2,600 y ago

Yannick Garcin^{a,1}, Pierre Deschamps^b, Guillemette Ménot^c, Geoffroy de Saulieu^d, Enno Schefuß^e, David Sebag^{f,g,h}, Lydie M. Dupont^e, Richard Oslisly^{d,i}, Brian Brademann^j, Kevin G. Mbusum^k, Jean-Michel Onana^{l,m}, Andrew A. Akoⁿ, Laura S. Epp^o, Rik Tjallingii^j, Manfred R. Strecker^a, Achim Brauer^j, and Dirk Sachse^p

^aInstitute of Earth and Environmental Science, University of Potsdam, 14476 Potsdam, Germany; ^bAix-Marseille Université, CNRS, IRD, Collège de France, Centre Européen de Recherche et d'Enseignement des Géosciences de l'Environnement UM34, 13545 Aix-en-Provence, France; ^cUniv Lyon, Ens de Lyon, Université Lyon 1, CNRS, UMR 5276 LGL-TPE, 69342 Lyon, France; ^dPatrimoines Locaux et Gouvernance UMR 208, IRD, MNHN, 75005 Paris, France; ^eMARUM—Center for Marine Environmental Sciences, University of Bremen, 28359 Bremen, Germany; ^fNormandie Université, UNIROUEN, UNICAEN, CNRS, M2C, 76000 Rouen, France; ^gHSM, LMI Picass'Eau, IRD, Université de Montpellier, 34095 Montpellier, France; ^hInstitute of Earth Surface Dynamics, Geopolis, University of Lausanne, 1015 Lausanne, Switzerland; ⁱAgence Nationale des Parcs Nationaux, 20379 Libreville, Gabon; ^jSection 5.2, Climate Dynamics and Landscape Evolution, GFZ—German Research Centre for Geosciences, 14473 Potsdam, Germany; ^kLaboratoire de Chimie de l'Environnement FRE 3416, Aix-Marseille Université, CNRS, 13545 Aix-en-Provence, France; ^lDepartment of Plant Biology, Faculty of Sciences, University of Yaoundé I, Yaoundé, Cameroon; ^mHerbier National du Cameroun, Institut de Recherche Agricole pour le Développement, Yaoundé, Cameroon; ⁿInstitute of Geological and Mining Research, Yaoundé, Cameroon; ^oAlfred Wegener Institute, Helmholtz Centre for Polar and Marine Research, 14473 Potsdam, Germany; and ^pSection 5.1, Geomorphology, GFZ—German Research Centre for Geosciences, 14473 Potsdam, Germany

Edited by Sarah J. Feakins, University of Southern California, Los Angeles, CA, and accepted by Editorial Board Member Ruth S. DeFries January 24, 2018 (received for review August 30, 2017)

A potential human footprint on Western Central African rainforests before the Common Era has become the focus of an ongoing controversy. Between 3,000 y ago and 2,000 y ago, regional pollen sequences indicate a replacement of mature rainforests by a forest–savannah mosaic including pioneer trees. Although some studies suggested an anthropogenic influence on this forest fragmentation, current interpretations based on pollen data attribute the “rainforest crisis” to climate change toward a drier, more seasonal climate. A rigorous test of this hypothesis, however, requires climate proxies independent of vegetation changes. Here we resolve this controversy through a continuous 10,500-y record of both vegetation and hydrological changes from Lake Barombi in Southwest Cameroon based on changes in carbon and hydrogen isotope compositions of plant waxes. $\delta^{13}\text{C}$ -inferred vegetation changes confirm a prominent and abrupt appearance of C_4 plants in the Lake Barombi catchment, at 2,600 calendar years before AD 1950 (cal y BP), followed by an equally sudden return to rainforest vegetation at 2,020 cal y BP. δD values from the same plant wax compounds, however, show no simultaneous hydrological change. Based on the combination of these data with a comprehensive regional archaeological database we provide evidence that humans triggered the rainforest fragmentation 2,600 y ago. Our findings suggest that technological developments, including agricultural practices and iron metallurgy, possibly related to the large-scale Bantu expansion, significantly impacted the ecosystems before the Common Era.

Western Central Africa | late Holocene | rainforest crisis | paleohydrology | human activity

Although the vast rainforests of Western Central Africa (WCA) are not considered pristine ecosystems (1), the influence of humans and climate change on their areal extent and composition during the past remains largely unknown. Over the last three decades, regional pollen sequences recovered from lakes and swamps have provided an unprecedented view of Holocene vegetation changes in the region. The most striking feature is a major vegetation disturbance that occurred between 3,000 calendar years before present (cal y BP) and 2,000 cal y BP (2–7). Although this vegetation disturbance appeared to be widespread across WCA (4), insufficient chronological control and sedimentary hiatuses have limited regional correlations or attribution to a single event (8). There is particularly strong evidence for the late Holocene rainforest crisis (LHRC) recorded in the sediments of Lake Barombi (or Barombi Mbo; 4° 39.6' N, 9° 24.3' E; Fig. 1). This sedimentary archive has

recorded a reversible switch from a mature rainforest to a disturbed/secondary forest, with a significant proportion of grasses and pioneer trees (3). This event was attributed to aridification associated with an increase in the duration of the dry season (3–5). An abrupt warming of sea surface temperatures (SSTs) in the Gulf of Guinea was inferred to have changed the monsoon precipitation (3, 5). Quantitative pollen-based reconstructions of mean annual precipitation of the Lake Barombi record were interpreted to reflect a 50% decrease in precipitation during the LHRC (9). Contemporaneous dry conditions were also inferred from nearby Lake Ossa using diatoms (10); however, a reanalysis of the sediments from this lake demonstrated a ~400-y age offset, due to the influence of aged soil carbon, and a dominant

Significance

Modern human societies live in strongly altered ecosystems. However, anthropogenic environmental disturbances occurred long before the industrial revolution. About 2,600 y ago, a forest–savannah mosaic replaced dense rainforests in Western Central Africa. This rainforest crisis was previously attributed either to the impact of climate change or, to a lesser extent, to the expansion of Bantu peoples through Central Africa. A 10,500-y sedimentary record from Lake Barombi, Southwest Cameroon, demonstrates that the rainforest crisis was not associated with any significant hydrological change. Based on a detailed investigation of a regional archaeological database, we present evidence that humans altered the rainforest ecosystem and left detectable traces in the sediments deposited in Lake Barombi.

Author contributions: Y.G. designed research; Y.G. coordinated research; Y.G., P.D., G.M., B.B., K.G.M., and A.A.A. performed fieldwork; Y.G. conducted sample preparation, chemical sample treatment, and stable hydrogen isotope analysis; E.S. carried out stable carbon isotope analysis; Y.G., G.d.S., and R.O. compiled and analyzed archaeological data; L.M.D. carried out pollen analysis; Y.G., P.D., G.M., G.d.S., E.S., D. Sebag, L.M.D., R.O., B.B., K.G.M., J.-M.O., A.A.A., L.S.E., R.T., M.R.S., A.B., and D. Sachse contributed to the interpretation and the discussion of the results; and Y.G. wrote the paper with contributions from all authors.

The authors declare no conflict of interest.

This article is a PNAS Direct Submission. S.J.F. is a guest editor invited by the Editorial Board.

Published under the [PNAS license](https://www.pnas.org/licenses).

Data deposition: The data reported in this paper have been deposited in the PANGAEA online database (<https://doi.pangaea.de/10.1594/PANGAEA.884676>).

¹To whom correspondence should be addressed. Email: yannickgarcin@yahoo.fr.

This article contains supporting information online at www.pnas.org/lookup/suppl/doi:10.1073/pnas.1715336115/-DCSupplemental.

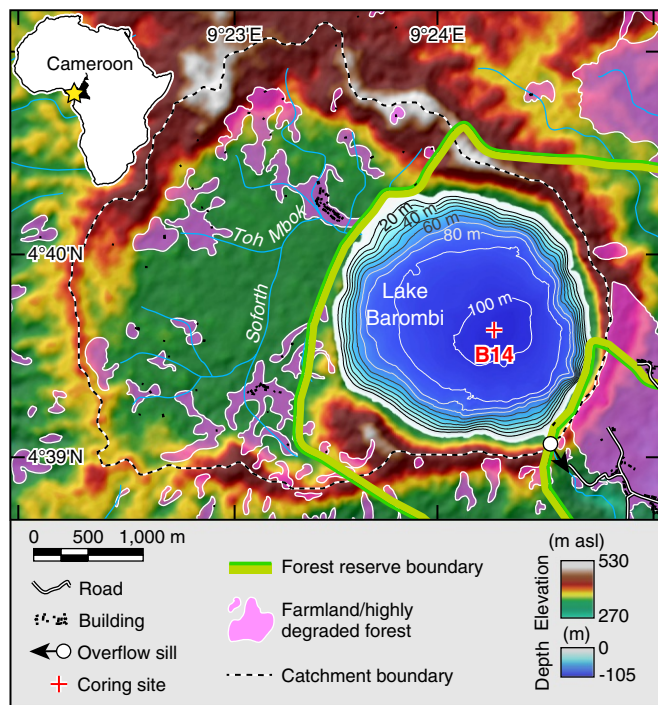


Fig. 1. Map of the Lake Barombi basin with topography, bathymetry (10-m contour intervals), and the coring site. Also highlighted are infrastructures and farmland/highly degraded forest based on SPOT 5 images and ArcGIS Online Basemap–World Imagery (source: Esri, DigitalGlobe, GeoEye, i-cubed, USDA, USGS, AEX, Getmapping, Aerogrid, IGN, IGP, swisstopo, and the GIS User Community). (*Inset*) Location map of Lake Barombi (yellow star) in Africa.

control of sedimentation by local forcing factors rather than regional climate, which have cast doubt on this assessment (11).

Although the LHRC is contemporaneous with a marked increase in human settlements and activity in the region (7, 12–16), it is generally assumed that humans at that time were not yet major agents of vegetation disturbances (4, 13, 15, 17–20). A recent study (21) suggesting that human land-use intensification associated with the southward migration of Bantu-speaking farmers across Central Africa contributed to forest destruction has, however, fueled a fierce debate in the paleoecology and archaeology communities (22, 23).

To support the notion of a climatic, i.e., hydrological driver of the LHRC, it is necessary to demonstrate independently that vegetation and hydrological changes were coeval, which has not been confirmed to date. Alternatively, to support anthropogenic impacts, changes in hydrological and vegetation proxies should be disconnected and unambiguous evidence of coeval human activity should be demonstrated.

Here we make use of the capability of stable carbon and hydrogen isotope ratios of plant wax-derived biomarkers to record both vegetation and hydrological changes independently in the same organic molecule (24, 25). We obtained a new 12-m-long sediment core from Lake Barombi (105-m water depth, Fig. 1) spanning the past 10,500 cal y BP. Our well-constrained age model is based on a total of 35 ^{14}C dates and on ^{210}Pb assay for the top of the sequence (*SI Appendix*). Paired carbon and hydrogen isotope compositions of the $n\text{-C}_{31}$ alkane ($\delta^{13}\text{C}_{n\text{-C}_{31}}$ and $\delta\text{D}_{n\text{-C}_{31}}$) were measured on 220 samples, providing an average temporal resolution of 50 y (Fig. 2).

Results

In Africa, $\delta^{13}\text{C}_{n\text{-C}_{31}}$ reflects the relative proportions of C_3 and C_4 plant waxes, which are produced by woody plants (trees/

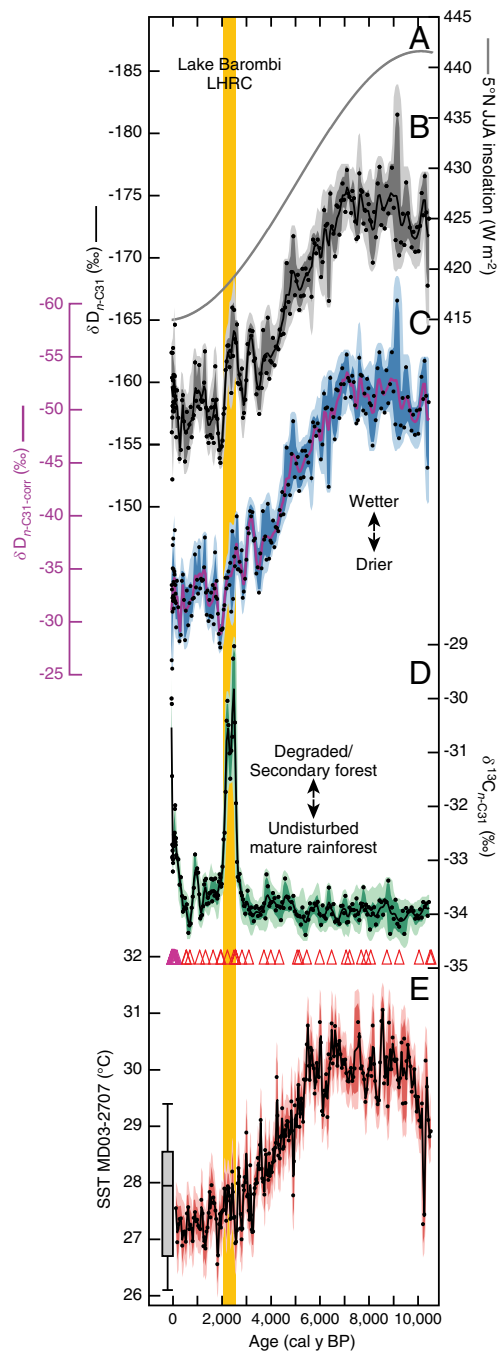


Fig. 2. Records of environmental change from Lake Barombi over the past 10,500 y and comparison with local summer insolation and Gulf of Guinea SSTs. (A) Long-term insolation changes at 5°N during Northern Hemisphere summer [June–July–August (JJA)] (40). (B) Lake Barombi $\delta\text{D}_{n\text{-C}_{31}}$. (C) Lake Barombi $\delta\text{D}_{n\text{-C}_{31}}$ corrected for vegetation changes ($\delta\text{D}_{n\text{-C}_{31}\text{-corr}}$). More positive (negative) values indicate drier (wetter) conditions. (D) Lake Barombi $\delta^{13}\text{C}_{n\text{-C}_{31}}$ reflecting vegetation changes, namely C_3 vs. C_4 plant contributions to sediments. $\delta^{13}\text{C}_{n\text{-C}_{31}}$ values have been corrected for the Suess effect for the last 160 y (*SI Appendix*). (D, Bottom) Purple and red triangles denote ^{210}Pb and ^{14}C dates, respectively, used in the Lake Barombi age model. (E) Mg/Ca-derived SST record from core MD03-2707 (41), reflecting ocean temperature changes in the Gulf of Guinea that were reassessed to account for the effect of changing salinity following ref. 42 (*SI Appendix*). The box plot indicates monthly modern SST values at the core site (43) (box shows the median, 25th and 75th percentiles; error bars are extended to extreme data points). (B–E) Single data points are denoted as dots; lines indicate median probabilities; envelopes reflect 68% (dark) and 95% (light) confidence intervals in the reconstructions, based on analytical and age model errors. Vertical yellow band indicates the timing of the Lake Barombi LHRC.

shrubs) and grasses, respectively (26–28). Although variation in relative humidity and light exposure can result in large variability in the $\delta^{13}\text{C}$ values of C_3 plants (28, 29), changes in $\delta^{13}\text{C}_{n-\text{C}_{31}}$ values in Lake Barombi sediments are positively correlated with the relative proportion of grass pollen and support their use to reconstruct the vegetation cover (SI Appendix). During most of the Holocene $\delta^{13}\text{C}_{n-\text{C}_{31}}$ remained stable, with values around -34‰ typical for an undisturbed, mature rainforest (Fig. 2D). However, a major excursion toward higher $\delta^{13}\text{C}_{n-\text{C}_{31}}$ values (up to -29‰) occurred between 2,600 cal y BP and 2,020 cal y BP (age uncertainties lower than 200 y at 95% confidence level). With a time span of probably less than 100 y, the lake catchment experienced a significant increase in C_4 plant cover mimicking the peak of grasses identified at lower resolution from pollen data (3) and bulk sediment $\delta^{13}\text{C}$ data (30). Our chronology indicates that the LHRC at Lake Barombi lasted ~ 600 y. Its inception and duration were ~ 300 y younger and ~ 400 y shorter than previously proposed (3). We argue that the LHRC at Lake Barombi was strongly amplified in the sedimentary record due to the high sensitivity of this small lake catchment to local vegetation changes. Subsequently, $\delta^{13}\text{C}_{n-\text{C}_{31}}$ fell back to low values, although slightly higher than pre-LHRC values, suggesting that the rainforest recovered, but never reached the maturity levels of the early and middle Holocene (3). Finally, toward the present day, $\delta^{13}\text{C}_{n-\text{C}_{31}}$

values record an increasing trend starting at ~ 500 cal y BP, which peaked during the last three decades, coeval with the recent acceleration of agriculture and deforestation in the lake catchment (Fig. 1).

In contrast to $\delta^{13}\text{C}$, which is a proxy indicator for vegetation, $\delta\text{D}_{n-\text{C}_{31}}$ values primarily record changes in the hydrogen isotope composition of precipitation (31). Stable isotope ratios in meteoric water in southwestern Cameroon are controlled by the amount of precipitation and the recycling of continental moisture (32, 33). On decadal timescales, the δD values of sedimentary plant waxes generally covary with the instrumental record of mean annual precipitation in West and Central Africa (ref. 34 and SI Appendix). In addition, $\delta\text{D}_{n-\text{C}_{31}}$ values can be modified by changes in evapotranspiration, amplifying isotopic change during aridification (31), as well as by different isotope fractionations associated with the changing vegetation. The latter effect can be accounted for using $\delta^{13}\text{C}_{n-\text{C}_{31}}$ (35–39) (see SI Appendix for more information). We note that the resulting vegetation correction of $\delta\text{D}_{n-\text{C}_{31}}$ is rather small (of up to 5‰) and has little influence on the hydroclimate signal (see $\delta\text{D}_{n-\text{C}_{31}-\text{corr}}$ in Fig. 2C). Based on the plant wax record, we detect the wettest conditions (lowest $\delta\text{D}_{n-\text{C}_{31}-\text{corr}}$) between 10,500 cal y BP and 7,000 cal y BP, followed by an uninterrupted, gradual drying trend lasting until 2,000 cal y BP. After this, the hydrology stabilized until the present day.

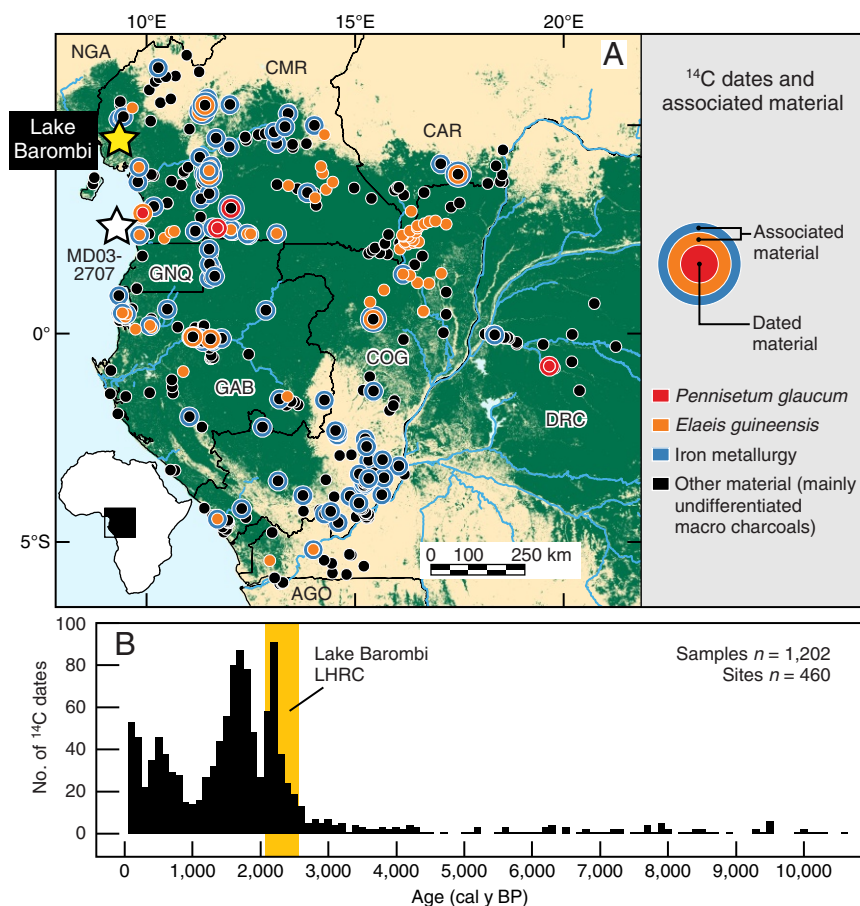


Fig. 3. Map of WCA, the Lake Barombi study site, and spatiotemporal distribution of 460 archaeological sites covering the past 10,500 y. (A) Current spatial distribution of rainforest shown in green, taken from the Collection 5 Moderate Resolution Imaging Spectroradiometer (MODIS) Global Land Cover Type product (www.landcover.org). (Inset) Map showing location of the study area in Africa. Countries: AGO, Angola; CAR, Central African Republic; CMR, Cameroon; COG, Republic of the Congo; DRC, Democratic Republic of the Congo; GAB, Gabon; GNQ, Equatorial Guinea; NGA, Nigeria. Overlain are ^{14}C -dated archaeological sites with dated and associated material as well as the location of Lake Barombi and marine core MD03-2707. (B) Number (No.) of ^{14}C -dated archaeological samples per 100-y period. Vertical yellow band indicates the timing of the Lake Barombi LHRC.

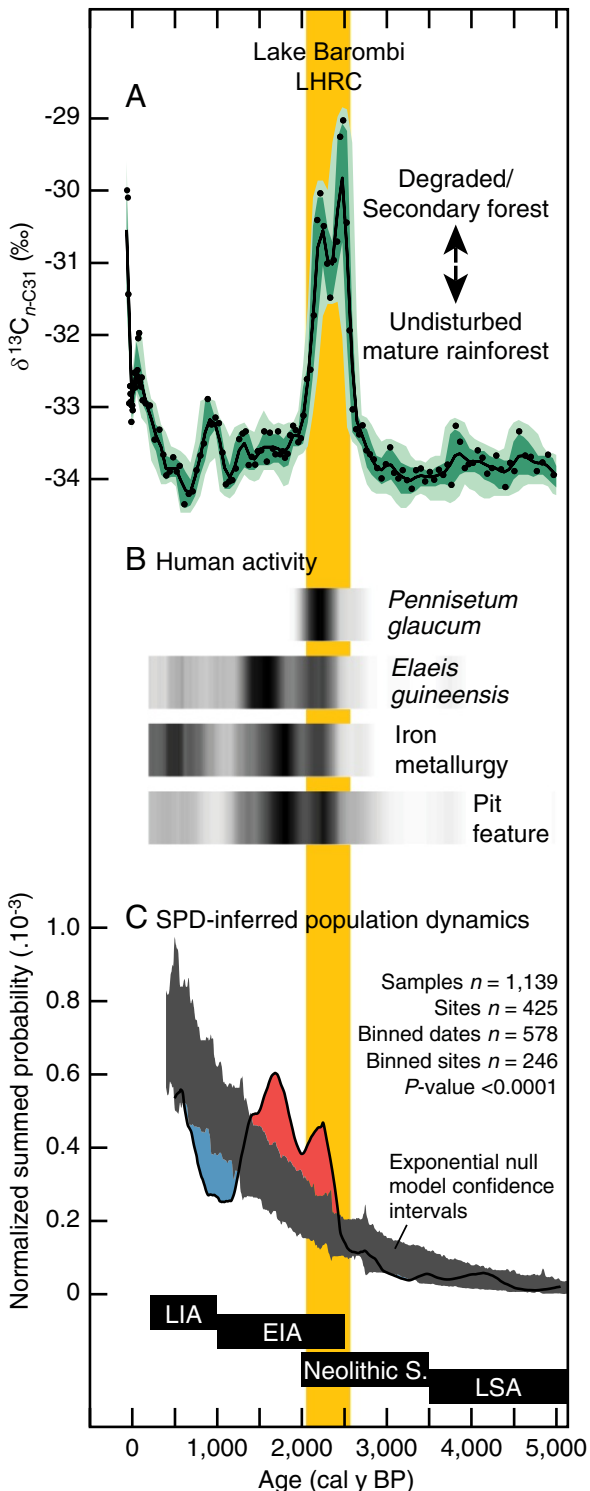


Fig. 4. Detailed comparison of the Lake Barombi vegetation changes and the archaeological record of WCA during the past 5,000 y. (A) Lake Barombi $\delta^{13}\text{C}_{n-C31}$ indicating vegetation changes. $\delta^{13}\text{C}_{n-C31}$ values have been corrected for the Suess effect for the last 160 y (SI Appendix). Dots are the raw measured data; line indicates median probability; envelopes reflect 68% (dark) and 95% (light) confidence intervals in the reconstruction, based on analytical and age model errors. (B and C) Archaeological synthesis of WCA. All presented archaeological data rely on the SPD of calibrated ^{14}C dates that were binned in space using 10-km radii and time using 200-y intervals (SI Appendix). SPDs were plotted with a 200-y moving average to prevent overinterpretation of smaller-scale variability (53–55) and are shown either as a gray scale [(B) black represents maximum probability, white represents

Discussion

The Lake Barombi plant wax record indicates a D enrichment during the Holocene interpreted as a drying signal. No such drying trend was evident from former pollen-based precipitation reconstructions from this site (9). This low-frequency variability suggests a dominant control of the Northern Hemisphere summer insolation on the isotopic composition of monsoon precipitation at orbital timescales (Fig. 2A). The timing of the drying at Lake Barombi differs from that at Lake Bosumtwi ($6^\circ 30' \text{ N}$) in West Africa, which recorded a reduction in precipitation from 9,000 cal y BP to 5,500 cal y BP, suggesting a regionally variable precipitation response to solar radiation (38).

In the Lake Barombi area, modern precipitation reaches $\sim 2,500 \text{ mm}\cdot\text{y}^{-1}$, which is sufficient to enable rainforest growth. Therefore, the vegetation remained relatively insensitive to the drying trend during the Holocene. Although late Holocene drier conditions led to increasing sensitivity to disturbances and a sustained switch from forest to savannah at the periphery of the former rainforest (15, 44, 45), the absence of any coeval drying (i.e., increase in $\delta\text{D}_{n-C31-\text{corr}}$) during the LHRC at Lake Barombi combined with the rapid regeneration of rainforest after 2,020 cal y BP does not support the primary climatic control on the LHRC that was previously proposed (3–6, 10, 13, 19). Additional evidence for the absence of any abrupt climatic change comes from the SST record of the nearby marine core MD03-2707 (41) (Fig. 2E and SI Appendix), since SST changes have been proposed as a potential trigger of a change in the seasonality of precipitation—that did not necessarily involve a change in the annual amount of precipitation—leading to the LHRC (3, 5, 6, 13, 19, 20). High temperatures of $\sim 30^\circ\text{C}$ occurred from 9,800 cal y BP to 5,600 cal y BP, followed by a progressive decrease to values of $\sim 27.5^\circ\text{C}$ at 200 cal y BP in close agreement with the modern mean SST value. Although the drying trend started $\sim 1,500$ y earlier than SST cooling, probably related to either different sensitivities of these records or spatial disparities between the integration areas of those signals, both climate proxies exhibit similar patterns. Based on this regional reference SST record, we are unable to detect any evidence for an abrupt SST change in the Gulf of Guinea associated with the LHRC, ruling out an oceanic control. Furthermore, marine records from the region do not show change in the hydrology at the time of the LHRC (41, 46). Further indications for limited hydrological change (including change in precipitation seasonality) during the LHRC are presented in SI Appendix.

Our results call for a reappraisal of the “anthropogenic hypothesis” (2, 21). To support this hypothesis, we reconstructed the temporal patterns of population dynamics and cultural change in WCA using a newly compiled database of 460 archaeological sites and 1,202 ^{14}C dates covering the last 10,500 y derived from ref. 47 (Figs. 3 and 4; see SI Appendix for detailed information). Before 4,000 cal y BP, dated archaeological sites were scarce and disparate in the study area. In contrast, coeval with the onset of the LHRC at Lake Barombi at 2,600 cal y BP, the number of dated archaeological sites increased abruptly (Fig. 3B). Based on the summed probability distribution (SPD) of

null probability] or as a line (C). (B) Evidence of human activity. (C) SPD-inferred population dynamics: SPD of ^{14}C dates (thick line) was compared against an exponential model used as a conservative null hypothesis reflecting both the long-term population rise observed in prehistoric populations and temporally increasing taphonomic loss (53–55) (SI Appendix). The dark gray area represents the 95% confidence intervals for the null model. Red and blue areas represent intervals with significant positive and negative deviations, respectively. Regional cultural timeline (13) shown at bottom (EIA, Early Iron Age; LIA, Late Iron Age; LSA, Late Stone Age; Neolithic S., Neolithic Stage). Vertical yellow band indicates the timing of the Lake Barombi LHRC.

calibrated ^{14}C dates from this database (Fig. 4C), we inferred a significant change (at 95% confidence level) in the archaeological record, highlighting a major positive deviation in population dynamics that occurred during the LHRC and that may be related to the Bantu expansion in WCA (7, 13, 19, 48–50). Starting from 3,000 cal y BP, sedentary Neolithic populations making pottery and carrying out pit features settled in WCA (13). At $\sim 2,400$ cal y BP, these populations began to cultivate pearl millet (*Pennisetum glaucum*), a C_4 crop; perform iron metallurgy; and use oil palm (*Elaeis guineensis*) (Fig. 4B). The termination of the Lake Barombi LHRC at $\sim 2,000$ cal y BP was synchronous with the disappearance of pearl millet in the archaeological record of WCA. Subsequently, from 2,000 cal y BP to 1,200 cal y BP, iron metallurgy as well as the use of oil palm culminated in WCA. This period also coincided with the second significant positive deviation in the archaeological record, which may have ended in a major demise of the population (ref. 13 and Fig. 4C).

We note that the inception of the LHRC as recorded at Lake Barombi occurred ~ 200 y earlier than the apparent establishment of technological developments in the whole of WCA (Fig. 4B). This difference in timing might either reflect chronological uncertainties or be an evidence of diffusion of people and/or technological developments related to the initial stage of the supposed expansion of Bantu-speaking peoples in WCA (51, 52) and associated disturbances.

On a local scale, our data suggest that humans practiced land clearing in the Lake Barombi basin during a major positive deviation in population dynamics associated with technological developments occurring at a regional scale that resulted in a local rainforest decline. The subsequent abandonment of the catchment or switch to agricultural practices with reduced impacts on vegetation could have fostered the regeneration of the rainforest.

Although humans probably triggered the LHRC in WCA, climate might have had an indirect role: In the drier regions north of the rainforest, concurrent late Holocene drying coupled with land degradation (56) may have encouraged populations to migrate southward, disseminating new technological developments into the rainforest.

Our results provide additional temporal and causal constraints on the current models of Bantu expansion—based on human genetic and linguistic phylogenies (19, 50, 57)—suggesting that the LHRC was the consequence rather than the cause of human dispersal in Central Africa.

Materials and Methods

This section presents the site description and a summary of methods, with full details provided in *SI Appendix*.

Study Site and Regional Climate. Lake Barombi is a 4.2-km², 105-m-deep, and circular (diameter of $\sim 2,300$ m) lake filling a volcanic maar crater. It is located 334 m above sea level, ~ 35 km to the northeast of Mt. Cameroon. It is an oligotrophic freshwater open lake overflowing into the Kumba River. Lake surface temperatures range from 26.7 °C to 29.5 °C (58). Below ~ 20 m the lake develops an anoxic hypolimnia (58). The Barombi maar is a polygenetic structure that formed through three eruptive cycles between ~ 510 kya and 80 kya (59). Phreatomagmatic explosions west of the Barombi maar resulted in the formation of an adjacent maar crater (59), which comprises most of the lake catchment area (10.4 km²) and is drained by a network

of small perennial rivers. The lake occupies the Barombi maar to the east, which is bowl shaped with steep slopes and a flat bottom. The local vegetation comprises lowland evergreen rainforest with patches of semideciduous forest (3, 60). A forest reserve was created in 1940 to protect the vegetation in the vicinity of the lake (61). Since ~ 30 y ago human impact related to farming and deforestation in the lake catchment strongly accelerated (62). The farming practice relies on mixed crops such as cocoyam, plantain, and maize and monocrop systems such as cocoa, oil palm, and rubber (61). Regional climate is controlled by the seasonal variability of the intertropical convergence zone (ITCZ) and its associated rain belt, which brings monsoonal precipitation from March to October. The mean annual rainfall at Kumba (town bordering the Lake Barombi catchment) is $\sim 2,500$ mm·y⁻¹, with monthly precipitation less than 100 mm·mo⁻¹ during 3–4 mo and a mean monthly temperature of 27 ± 2 °C (63).

Sediment Core. In January 2014 core B14 was collected in the deepest (105 m deep) and central part of Lake Barombi from a UWITEC hybrid floating platform using a UWITEC percussion piston coring system. Based on previous studies of the Lake Barombi sediments (3, 30, 64, 65) we focused our analyses on the first 12 m of sediments, which represent the Holocene Epoch. A continuous 11.71-m-long composite sequence was constructed from holes B14-2 and B14-5 after core splitting based on lithological features (*SI Appendix, Fig. S1*). Event deposits (turbidites and tephras) were excised from the original composite depth scale, resulting in an event-free 9.94-m-long depth scale. Based on 21 ^{210}Pb dates and 35 ^{14}C dates (*SI Appendix, Tables S1–S3*) we generated an age model for the Lake Barombi event-free sediment record (*SI Appendix, Figs. S2 and S3*) using Bayesian approaches, as implemented in the freely available R statistical computing package Bacon v2.2 (66, 67) and using the Southern Hemisphere calibration curve SHCal13 (68).

Molecular and Isotopic Analyses. Core B14 was sampled continuously with contiguous 1-cm slabs for the topmost 25 cm of the sequence and contiguous 5-cm slabs for the rest of the sequence. Components of terrestrial plant waxes were extracted from freeze-dried lacustrine sediments using an accelerated solvent extractor with a dichloromethane/methanol mixture of 9:1. The *n*-alkanes were isolated over a solid phase extraction on silica gel and then purified. They were identified by gas chromatography mass spectrometry using a flame ionization detector and quantified by comparison with an internal standard and standard mixtures of *n*-C₁₀–*n*-C₄₀ alkanes. Carbon and hydrogen isotope ratios (*SI Appendix, Fig. S4*) were measured using gas chromatography coupled to an isotope ratio mass spectrometer, using a combustion interface (for $\delta^{13}\text{C}$) and a pyrolysis furnace (for δD). Carbon and hydrogen isotope values were corrected based on values of isotopic standards and are reported on the Vienna Pee Dee Belemnite and Vienna Standard Mean Ocean Water scales, respectively.

ACKNOWLEDGMENTS. We thank the Barombi people and their Chief J. S. Ndokpe as well as the administrative authorities of Cameroon for support and collaboration during fieldwork. We thank T. Klaka-Tauscher and M. Elomo Molo (logistics); R. Niederreiter (core collection); M. Pöhle, M. Patyniak, X. Hadeen, and T. Syla (sample processing); G. Zeilinger (help with GIS analysis); B. Ghaleb (^{210}Pb analyses); and E. R. Crema (help with SPD modeling of calibrated ^{14}C dates). We also thank an anonymous reviewer and K. Uno for their helpful comments on the manuscript. Fieldwork was conducted with research permission of the Ministry of Scientific Research and Innovation of Cameroon. SPOT satellite images (©CNES) were acquired through the ISIS-888 Project. We acknowledge the French National Research Institute for Sustainable Development (IRD), its local office in Yaoundé, and the LMI DYCOFAC for their support. This work was supported by the Deutsche Forschungsgemeinschaft (DFG) (Grant GA1629/2 to Y.G.). Y.G. and M.R.S. were also supported by the Ministry of Science, Research, and Culture des Landes Brandenburg. P.D. was supported by Labex OT-Med and EQUIPEX ASTER-CEREGE projects. G.M. acknowledges the BNP-Paribas Climate Initiative Foundation (Project CPATEMP). E.S. and L.M.D. were supported by the DFG-Research Center/Cluster of Excellence “The Ocean in the Earth System” at MARUM—Center for Marine Environmental Sciences.

- van Gemerden BS, Olff H, Parren MPE, Bongers F (2003) The pristine rain forest? Remnants of historical human impacts on current tree species composition and diversity. *J Biogeogr* 30:1381–1390.
- Richards K (1986) *Preliminary Results of Pollen Analysis of a 6000 year Core from Mboandong, a Crater Lake in Cameroon*, Geography Department Miscellaneous Series No. 32 (Univ of Hull, Hull, UK).
- Maley J, Brenac P (1998) Vegetation dynamics, palaeoenvironments and climatic changes in the forests of western Cameroon during the last 28,000 years BP. *Rev Palaeobot Palynol* 99:157–187.
- Vincens A, et al. (1999) Forest response to climate changes in Atlantic Equatorial Africa during the last 4000 years BP and inheritance on the modern landscapes. *J Biogeogr* 26:879–885.
- Maley J (2002) A catastrophic destruction of African forests about 2,500 years ago still exerts a major influence on present vegetation formations. *IDS Bull* 30:13–30.
- Ngomanda A, Neumann K, Schweizer A, Maley J (2009) Seasonality change and the third millennium BP rainforest crisis in southern Cameroon (Central Africa). *Quat Res* 71:307–318.

7. Neumann K, et al. (2012) First farmers in the Central African rainforest: A view from southern Cameroon. *Quat Int* 249:53–62.
8. Bonnefille R (2011) Rainforest responses to past climatic changes in tropical Africa. *Tropical Rainforest Responses to Climatic Change*, eds Bush MB, Flenley JR, Gosling WD (Springer Praxis, Chichester, UK), pp 125–184.
9. Lebamba J, Vincens A, Maley J (2012) Pollen, vegetation change and climate at Lake Barombi Mbo (Cameroon) during the last ca. 33 000 cal yr BP: A numerical approach. *Clim Past* 8:59–78.
10. Nguetsop VF, Servant-Vildary S, Servant M (2004) Late Holocene climatic changes in west Africa, a high resolution diatom record from equatorial Cameroon. *Quat Sci Rev* 23:591–609.
11. Debret M, et al. (2014) Influence of inherited paleotopography and water level rise on the sedimentary infill of Lake Ossa (S Cameroon) inferred by continuous color and bulk organic matter analyses. *Palaeogeogr Palaeoclimatol Palaeoecol* 411:110–121.
12. Sowunmi MA (1999) The significance of the oil palm (*Elaeis guineensis* Jacq.) in the late Holocene environments of west and west central Africa: A further consideration. *Veget Hist Archaeobot* 8:199–210.
13. Oslisly R, et al. (2013) Climatic and cultural changes in the west Congo Basin forests over the past 5000 years. *Philos Trans R Soc Lond Ser B* 368:20120304.
14. Morin-Rivat J, et al. (2016) High spatial resolution of late-Holocene human activities in the moist forests of central Africa using soil charcoal and charred botanical remains. *Holocene* 26:1954–1967.
15. Lézine AM, et al. (2013) Temporal relationship between Holocene human occupation and vegetation change along the northwestern margin of the Central African rainforest. *C R Geosci* 345:327–335.
16. Wotzka H (2006) Records of activity: Radiocarbon and the structure of iron age settlement in central Africa. *Grundlegungen. Beiträge zur Europäischen und Afrikanischen Archäologie für Manfred K. H. Eggert*, ed Wotzka H (Francke, Tübingen, Germany), pp 271–289.
17. Schwartz D (1992) Assèchement climatique vers 3000 B.P. et expansion Bantu en Afrique centrale: Quelques réflexions. [Climatic drying about 3,000 B.P. and Bantu expansion in Atlantic Central Africa: Some reflections]. *Bull Soc Géol Fr* 163:353–361. French.
18. Brncic TM, Willis KJ, Harris DJ, Washington R (2007) Culture or climate? The relative influences of past processes on the composition of the lowland Congo rainforest. *Philos Trans R Soc Lond Ser B* 362:229–242.
19. Bostoen K, et al. (2015) Middle to late Holocene paleoclimatic change and the early Bantu expansion in the rain forests of western central Africa. *Curr Anthropol* 56:354–384.
20. Maley J, et al. (2018) Late Holocene forest contraction and fragmentation in central Africa. *Quat Res* 89:43–59.
21. Bayon G, et al. (2012) Intensifying weathering and land use in iron age Central Africa. *Science* 335:1219–1222.
22. Maley J, Giresse P, Doumenge C, Favier C (2012) Comment on “Intensifying weathering and land use in iron age Central Africa”. *Science* 337:1040.
23. Neumann K, et al. (2012) Comment on “Intensifying weathering and land use in iron age Central Africa”. *Science* 337:1040.
24. Schefuß E, Schouten S, Schneider RR (2005) Climatic controls on central African hydrology during the past 20,000 years. *Nature* 437:1003–1006.
25. Tierney JE, Russell JM, Huang Y (2010) A molecular perspective on late quaternary climate and vegetation change in the Lake Tanganyika basin, East Africa. *Quat Sci Rev* 29:787–800.
26. Rommerskirchen F, Plader A, Eglinton G, Chikaraishi Y, Rullkötter J (2006) Chemotaxonomic significance of distribution and stable carbon isotopic composition of long-chain alkanes and alkan-1-ols in C_4 grass waxes. *Org Geochem* 37:1303–1332.
27. Vogts A, Moossen H, Rommerskirchen F, Rullkötter J (2009) Distribution patterns and stable carbon isotopic composition of alkanes and alkan-1-ols from plant waxes of African rain forest and savanna C_3 species. *Org Geochem* 40:1037–1054.
28. Garcin Y, et al. (2014) Reconstructing C_3 and C_4 vegetation cover using n-alkane carbon isotope ratios in recent lake sediments from Cameroon, Western Central Africa. *Geochim Cosmochim Acta* 142:482–500.
29. Graham HV, et al. (2014) Isotopic characteristics of canopies in simulated leaf assemblages. *Geochim Cosmochim Acta* 144:82–95.
30. Giresse P, Maley J, Brenac P (1994) Late Quaternary palaeoenvironments in the Lake Barombi Mbo (West Cameroon) deduced from pollen and carbon isotopes of organic matter. *Palaeogeogr Palaeoclimatol Palaeoecol* 107:65–78.
31. Sachse D, et al. (2012) Molecular paleohydrology: Interpreting the hydrogen-isotopic composition of lipid biomarkers from photosynthesizing organisms. *Annu Rev Earth Planet Sci* 40:221–249.
32. Njitchoua R, et al. (1999) Variations of the stable isotopic compositions of rainfall events from the Cameroon rain forest, Central Africa. *J Hydrol* 223:17–26.
33. Wirmvem MJ, et al. (2016) Variation in stable isotope ratios of monthly rainfall in the Douala and Yaounde cities, Cameroon: Local meteoric lines and relationship to regional precipitation cycle. *Appl Water Sci* 7:2343–2356.
34. Niedermeyer EM, et al. (2016) The stable hydrogen isotopic composition of sedimentary plant waxes as quantitative proxy for rainfall in the West African Sahel. *Geochim Cosmochim Acta* 184:55–70.
35. Collins JA, et al. (2013) Estimating the hydrogen isotopic composition of past precipitation using leaf-waxes from western Africa. *Quat Sci Rev* 65:88–101.
36. Feakins SJ (2013) Pollen-corrected leaf wax D/H reconstructions of northeast African hydrological changes during the late Miocene. *Palaeogeogr Palaeoclimatol Palaeoecol* 374:62–71.
37. Magill CR, Ashley GM, Freeman KH (2013) Water, plants, and early human habitats in eastern Africa. *Proc Natl Acad Sci USA* 110:1175–1180.
38. Shanahan TM, et al. (2015) The time-transgressive termination of the African humid period. *Nat Geosci* 8:140–144.
39. Tierney JE, Pausata FSR, deMenocal PB (2017) Rainfall regimes of the Green Sahara. *Sci Adv* 3:e1601503.
40. Laskar J, et al. (2004) A long-term numerical solution for the insolation quantities of the Earth. *Astron Astrophys* 428:261–285.
41. Weldeab S, Lea DW, Schneider RR, Andersen N (2007) Centennial scale climate instabilities in a wet early Holocene West African monsoon. *Geophys Res Lett* 34:L24702.
42. Thirumalai K, Quinn TM, Marino G (2016) Constraining past seawater $\delta^{18}O$ and temperature records developed from foraminiferal geochemistry. *Paleoceanography* 31:1409–1422.
43. Levitus S, Boyer T (1994) *World Ocean Atlas 1994, Temperature*, NOAA Atlas NESDIS 4 (US Government Printing Office, Washington, DC).
44. Vincens A, Buchet G, Servant M, ECOFIT Mbalang Collaborators (2010) Vegetation response to the “African humid period” termination in Central Cameroon ($7^{\circ}N$) – new pollen insight from Lake Mbalang. *Clim Past* 6:281–294.
45. Lebamba J, Vincens A, Lézine AM, Marchant R, Buchet G (2016) Forest-savannah dynamics on the Adamawa plateau (Central Cameroon) during the “African humid period” termination: A new high-resolution pollen record from Lake Tizong. *Rev Palaeobot Palynol* 235:129–139.
46. Collins JA, et al. (2017) Rapid termination of the African humid period triggered by northern high-latitude cooling. *Nat Commun* 8:1372.
47. de Saulieu G, et al. (2017) Plateforme des datations archéologiques d’Afrique Centrale, Version 2.0. Available at vmtropical-proto.ird.fr/archeologie/afrique. Accessed March 31, 2017.
48. Vansina J (1984) Western Bantu expansion. *J Afr Hist* 25:129–145.
49. Russell T, Silva F, Steele J (2014) Modelling the spread of farming in the Bantu-speaking regions of Africa: An archaeology-based phylogeography. *PLoS One* 9:e87854.
50. Grollemund R, et al. (2015) Bantu expansion shows that habitat alters the route and pace of human dispersals. *Proc Natl Acad Sci USA* 112:13296–13301.
51. Vansina J (1990) *Paths in the Rainforests: Toward a History of Political Tradition in Equatorial Africa* (Univ of Wisconsin Press, Madison, WI).
52. Phillipson D (2005) *African Archaeology* (Cambridge Univ Press, New York).
53. Shennan S, et al. (2013) Regional population collapse followed initial agriculture booms in mid-Holocene Europe. *Nat Commun* 4:2486.
54. Timpson A, et al. (2014) Reconstructing regional population fluctuations in the European Neolithic using radiocarbon dates: A new case-study using an improved method. *J Archaeol Sci* 52:549–557.
55. Crema E, Habu J, Kobayashi K, Madella M (2016) Summed probability distribution of ^{14}C dates suggests regional divergences in the population dynamics of the Jomon period in eastern Japan. *PLoS One* 11:e0154809.
56. Höhn A, Neumann K (2016) The palaeovegetation of Janruwa (Nigeria) and its implications for the decline of the Nok culture. *J Afr Archaeol* 14:331–353.
57. Patin E, et al. (2017) Dispersals and genetic adaptation of Bantu-speaking populations in Africa and North America. *Science* 356:543–546.
58. Kling GW (1988) Comparative transparency, depth of mixing, and stability of stratification in lakes of Cameroon, West-Africa. *Limnol Oceanogr* 33:27–40.
59. Tchamabé B, et al. (2014) Temporal evolution of the Barombi Mbo maar, a polygenetic maar–diatreme volcano of the Cameroon volcanic line. *Int J Geosci* 5:1315–1323.
60. Letouzey R (1985) *Notice de la Carte Phytogéographique du Cameroun au 1:500 000* (Institut de la Carte Internationale de la Végétation, Toulouse, France).
61. Tchouto Mbatouh G, Essoung E, Mbong K (2015) *Socioeconomic Survey of The Lake Barombi Mbo Forest Reserve, South West Region, Cameroon* (Programme for the Sustainable Management of Natural Resources in the South West Region of Cameroon, Buea, Cameroon).
62. Giresse P, Maley J, Ngos S (2000) Source et puits du carbone dans le Sud-Cameroun, enregistrements lacustres et évolution à long terme. *Dynamique à Long Terme des Écosystèmes Forestiers Intertropicaux*, eds Servant M, Servant Vildary S (IRD, UNESCO, Paris), pp 149–157.
63. Suchel J (1987) *Les climats du Cameroun*. PhD dissertation (Univ of Bordeaux III, Bordeaux, France).
64. Giresse P, Maley J, Kelts K (1991) Sedimentation and palaeoenvironment in crater lake Barombi Mbo, Cameroon, during the last 25,000 years. *Sediment Geol* 71:151–175.
65. Cornet G, Bande Y, Giresse P, Maley J (1992) The nature and chronostratigraphy of Quaternary pyroclastic accumulations from lake Barombi Mbo (West-Cameroon). *J Volcanol Geotherm Res* 51:357–374.
66. Blaauw M, Christen JA (2011) Flexible paleoclimate age-depth models using an autoregressive gamma process. *Bayesian Anal* 6:457–474.
67. R Core Team (2013) *R: A Language and Environment for Statistical Computing* (R Foundation for Statistical Computing, Vienna). Available at www.R-project.org/. Accessed November 20, 2016.
68. Hogg AG, et al. (2013) SHCal13 Southern Hemisphere calibration, 0–50,000 years cal BP. *Radiocarbon* 55:1889–1903.